

## Seismic waves radiated from nonlinear vibration source and prevision of earthquakes

KIKUCHI, Toshiaki<sup>1\*</sup>

<sup>1</sup>National defense academy

This study describes the vibration characteristics of hypocenters using actual data and methods used in sound vibration analysis. Recent earthquakes near Mt. Fuji are used to analyze the earthquake hypocenter vibrations. Earthquakes larger than M5.0 occurred four times between 2009 and 2012 in this area. Earthquake signals were processed using the time-reversal method and simulated to obtain the time-reversal pulse. The frequency of the time-reversal pulse depends on the azimuth. The peak frequency is the frequency of the maximum frequency spectrum; it too depends on the azimuth. These dependencies are caused by nonlinear acoustic radiation in active faults. Such phenomena suggest that the vibration source moves at a high speed similar to a parametric source, which suggests the existence of points with unique spectra along the radiation direction, owing to parametric effects, i.e., the so-called parametric spots.

Further, these observations were common in the precursor earthquakes, the main shock, and the aftershocks. Hence, a dynamic model for the nonlinear vibration of the hypocenter is proposed. The model is verified by using actual earthquake data and is expected to find application in earthquake prediction by observing the waveforms of weak earthquakes.

Pavlov et al. examined nonlinear vibrations in an inhomogeneous medium and derived the equation for the Cerenkov radiation and transition radiation. The Cerenkov radiation is generated in a narrow angular range of the traveling direction near the source and the waveform is pulse-like. The transition radiation depends on the angle. The narrow beam at the radiation end has the same characteristic as the Cerenkov radiation. The peak frequency is also a function of the angle at the radiation end. On the other hand, the inhomogeneous medium structure constants are not well known. However, because the peak frequency patterns with respect to azimuth are similar for the earthquakes, the abovementioned phenomena are considered specific to the hypocenter vibrations. The earthquake data are from the Hi-net of National Research Institute for Disaster Prevention.

Keywords: Hypocenter vibration, Time reversal, Waveform of seismic wave, Transition radiation, Seismic wave propagation, Prevision of earthquakes

## Tsunami observation inside the source region: a simulation and a theory

SAITO, Tatsuhiko<sup>1\*</sup>

<sup>1</sup>National Research Institute for Earth Science and Disaster Prevention

A tsunami observation network is being constructed offshore northeastern Japan, where ~150 ocean-bottom seismometers and pressure gauges are to be deployed across the source area of huge earthquakes that could possibly occur in future. Since tsunami records inside the source region are seriously contaminated by ocean-acoustic and seismic waves, we cannot correctly estimate the tsunami size if conventional methods are directly used in analyzing these records. It is fundamentally important to know the contributions of the acoustic wave and sea-bottom movements on the tsunami records. By numerically simulating the tsunami generation from the earthquake rupture including the interactions between fluid ocean and elastic earth medium (e.g. Maeda and Furumura 2013 PAGEOPH), we investigated the relation between the sea-bottom pressure and the sea-bottom motion. Past studies employed a simple relation  $p = \rho a h$  for interpreting ocean-bottom pressure records (e.g. Filloux 1982 GRL), where  $p$  is the pressure generated by dynamic sea-bottom deformation,  $a$  is the acceleration of the sea bottom,  $\rho$  is the water density, and  $h$  is the sea depth. However, our simulations indicated that this relation failed when a steep sea-bottom deformation occurred. It was necessary to extend the relation by using an analytical solution of an incompressible fluid theory (Saito 2013 EPS). We confirmed that a spatial filtering of  $\tanh(kh)/kh$  in the wavenumber domain  $k$  reproduced our simulation results better than the simple relation in the past studies.

Keywords: tsunami, earthquake fault, seismic wave, ocean acoustic wave

## The crust and mantle heterogeneities beneath Japanese Islands investigated by the Hi-net and wave propagation simulation

FURUMURA, Takashi<sup>1\*</sup>

<sup>1</sup>CIDIR/ERI The Univ. Tokyo

### 1. Background

Regional seismic wavefield observed in the Hi-net high-density seismic network deployed over Japanese Islands is investigated by comparison between compute simulation of seismic wave propagation using recent high-resolution velocity and attenuation tomography models. It is expected that the regional wavefield is strongly influenced by heterogeneities in the crust and upper-mantle structure along propagation path. For example, mantle Pn and Sn wave is very sensitive to the super/sub Moho structure, and the Rg wave is influenced by near-surface structure. Moreover, the crustally guided Lg wave is sensitive to the roughness of surface and Moho interface and heterogeneities in the crustal structure. Thus, by make full use of these regional phases, it is expecting to investigate the heterogeneities and regionalities of the crust and upper-mantle structure in Japan.

### 2. Data and Method

The Hi-net data for intermediate (M4-5) scale and shallow ( $H < 40\text{km}$ ) earthquakes was used in this study to investigate the regionalities of the seismic wave propagation in Japan especially the difference in the wavefield between northeastern and southwestern Japan where strong difference in the crust/mantle structure is expected. The FDM simulation of seismic wave propagation was conducted using the velocity (Matsubara et al., 2008) and attenuation tomography (Sekine, 2001; Nakamura, 2008) models. In order to examine the scattering of high-frequency ( $f > 1\text{ Hz}$ ) seismic wavefield, small-scale heterogeneities which is described by vonKarman distribution function with horizontal and vertical correlation length of  $A_{x,y}/A_z = 10/0.5\text{ km}$  and standard deviation of  $e = 1-2\%$  which is based on former studies (Furumura and Kennett, 2005; Furumura et al., 2014) is superposed on the tomography model and made a *Hybrid heterogeneity model*.

### 3. Results

Based on the analysis of dense Hi-net seismic data over Japan and computer simulation of seismic wave propagation, it is obtained the following conclusions about the characteristics of the regional wavefield in Japan:

(1) The amplitude of the Sn wave is large in southwestern Japan (compared with northeastern Japan). This is because; 1) the velocity gradient in the sub-Moho structure push up S wave energy from the mantle to the crust which develop large Sn phase, 2) a larger Qs in the mantle develop large Sn phase for longer distances.

(2) The attenuation of the Lg wave is large in northeastern Japan (compared with southwestern Japan). This is because; 1) strong Lg-to-P conversion occurs in the low-wavespeed superficial layer remove Lg wave energy, 2) a larger Qs in the crust o northeastern Japan especially beneath volcano attenuate Lg very drastically, 3) a smaller velocity contrast across Moho leaks S wave energy into the mantle.

(3) A larger Pg is observed in northeastern Japan. This is because; 1) a low-wavespeed superficial layer suppressing generation of the P-to-S conversion and leasing large Pg wave propagating in the crust by multiple reflections.

(4) Attenuation of the short-period surface (Rg) wave is large in northeastern Japan. This is because; 1) strong dispersion and elongation of surface wave occurs in the surface wave due to the existence of low-velocity superficial layer in northeastern Japan, 2) strong attenuation occurs in the short-period surface waves as propagating in low-Q crust.

## Three dimensional seismic wave-speed structure beneath the Kanto Plain based on adjoint tomography

MIYOSHI, Takayuki<sup>1\*</sup> ; OBAYASHI, Masayuki<sup>1</sup> ; TONO, Yoko<sup>1</sup> ; ANDO, Kazuto<sup>1</sup> ; TSUBOI, Seiji<sup>1</sup>

<sup>1</sup>JAMSTEC

We have obtained the preliminary model of three dimensional (3D) structure beneath the Kanto Plain, metropolitan area of Japan. We applied the spectral-element method (e.g. Peter et al. 2011) and adjoint method (Liu and Tromp 2006) to infer 3D velocity model and to reproduce the observed waveform bandpass filtered between 5 and 20 second. We used the travel-time tomography result (Matsubara and Obara 2011) as an initial 3D model and used broadband records obtained at the NIED F-net stations. We selected 147 earthquakes based on the earthquake catalog by the F-net and the S/N ratio of their seismograms. The 3D model used for the forward and adjoint simulations is represented as a region of approximately 500 by 450 km in horizontal and 120 km in depth. Minimum period was 4 sec. The initial 3D model reproduced P-wave seismograms well, however it could not really explain S-waves and later arrivals. For the adjoint inversion, we picked up the windows of the body waves from the observed and theoretical seismograms. The forward and adjoint simulations were implemented by K computer in RIKEN. The performance of the original application was 5% of the peak performance of the K computer, however the modified code achieved 10% by optimization. One iteration requires about 0.1 million CPU hours at least. The model parameters of Vp and Vs were updated by using the steepest descent method. The revised model reproduces observed waveforms better than the initial model. Acknowledgements: This research was partly supported by MEXT Strategic Program for Innovative Research. We thank to Dr. Daniel Peter for his comments and suggestions. We also thank to the NIED for providing seismological data.

Keywords: Kanto Plain, seismic wave-speed structure, adjoint tomography

## S wave attenuation and high-frequency seismic wavefield at Taal volcano, Philippines, inferred from waveform simulations

MORIOKA, Hanae<sup>1\*</sup> ; KUMAGAI, Hiroyuki<sup>1</sup> ; MAEDA, Takuto<sup>2</sup> ; MAEDA, Yuta<sup>1</sup>

<sup>1</sup>Graduate School of Environmental Studies, Nagoya University, <sup>2</sup>Earthquake Research Institute, the University of Tokyo

Taal volcano is one of the world's most active volcanoes. The existence of a region of strong attenuation (a low-Q region) near the ground surface, which may represent degassing magma, was estimated at Taal volcano, Philippines, from source location analysis using the amplitude source location (ASL) method. The ASL method uses high-frequency amplitudes under the assumption of isotropic S wave radiation caused by the scattering of seismic waves. To investigate the validity of the estimated Q structure based on a stochastic approach of the ASL method and to understand the nature of seismic wavefield, we used a deterministic approach based on numerical simulations of high-frequency seismic waveforms. We synthesized waveforms of volcano-tectonic events at Taal using a 3-D finite-difference method. We used focal mechanisms derived from first-motion polarities, and examined various sizes of Q anomalies, in which P and S wave velocities and density were assumed to be constant. To evaluate the fits between the observed and synthesized waveforms, we calculated the normalized residual using mean amplitudes in four frequency bands (1-6, 3-8, 5-10, and 7-12 Hz). Our simulations provided the minimum residual when using the low-Q region estimated by the ASL method. Although our simulation is a deterministic approach and different from the stochastic approach of the ASL method, the low-Q region estimated from these approaches was coincident. There were possible focal mechanisms for each VT event because they were derived from first-motion polarities at a small number of stations. We found that the residuals depended on assumed focal mechanisms. If the radiation pattern of the observed waveforms is isotropic, it is expected that the residuals do not depend on mechanisms. The coincidence of the estimated low-Q region and the residual dependence on focal mechanisms indicate that the radiation pattern of the observed waveforms in a high-frequency band is not completely isotropic and is also affected by focal mechanisms.

Keywords: Q factor, Magma, Amplitude source location method, Finite-difference method, Radiation pattern

## Scheme for computing seismic wave propagation in a 3D round sub-global earth model

TAKENAKA, Hiroshi<sup>1\*</sup> ; TOYOKUNI, Genti<sup>2</sup> ; NAKAMURA, Takeshi<sup>3</sup> ; KOMATSU, Masanao<sup>1</sup> ; OKAMOTO, Taro<sup>4</sup>

<sup>1</sup>Graduate School of Natural Science and Technology, Okayama University, <sup>2</sup>Graduate School of Science, Tohoku University, <sup>3</sup>Japan Agency for Marine-Earth Science and Technology, <sup>4</sup>Graduate School of Science and Engineering, Tokyo Institute of Technology

We propose a "quasi-Cartesian" finite-difference scheme to compute seismic wave propagation for a very large region model of sub-global scale beyond regional and less than global ones, where the effects of roundness of Earth. This new scheme solves the elastodynamic equations for three-dimensionally heterogeneous (3D) spherical earth model in the "quasi-Cartesian" coordinate system similar to a local Cartesian system, instead of the spherical coordinate system, with a staggered finite-difference method (FDM) which is the most popular in seismic motion simulations for local to regional scale models. The developed scheme can be easily implemented in 3D Cartesian FDM codes by changing a very small part of the codes. It may be able to open a window for multi-scale modelling of seismic wave propagation in scales from sub-global to local one.

Keywords: seismic wave, simulation, finite-difference method

## Hyper resonance in the southern part of the Boso Peninsula for a period of 15 s to 20 s

KAWASAKI, Ichiro<sup>1\*</sup>; NISHIMURA, Takuya<sup>2</sup>; ISHII, Hiroshi<sup>1</sup>; ASAI, Yasuhiro<sup>1</sup>

<sup>1</sup>Tono Research Institute of Earthquake Science, <sup>2</sup>Disaster Prevention Research Institute, Kyoto University

### 1. The Mw8.4 super sub-event associated with the 2011 Mw9 Tohoku earthquake

Analyzing GPS high sampling displacement records of the 2011 Tohoku earthquake, Kawasaki et al. (2014) showed the followings:

The most dominant phase was the main pulse of a width of around 100 s and amplitude of a few meters in the Tohoku district (epicentral distances from 100 km to 350 km). An overall feature of the main pulse was explained by a simple rectangular fault model of low angle thrusting, which started about 35 s after the JMA origin time and released an interplate moment corresponding to Mw9.

The second was the "sub-pulse" (SH wave). Fig.1 shows record sections of transverse component of the GPS high sampling records for every 5 degree from N135W to N155W in the Kanto District (epicentral distance of 420-460 km). The distinguished pulse between two vertical broken lines at 65 s and 95 s was the sub-pulse of a width of around 30 s and amplitude of up to 1 meter. An overall feature of the sub-pulse was fitted by an Mw8.4 super sub-event fault model of strike slip faulting on nearly vertical plane striking in N140E direction.

### 2. Hyper resonance of a period of 15 s to 20s

The most remarkable phase following the sub-pulse is the hyper resonance (HR-1), which is a phase of a few cycles with a period of 15-20 s and peak-to-peak amplitude of up to 1 m in azimuths of N140W-N145W and N145W-N150W. The hyper resonance could be attributed to the Tertiary accretionary layer.

About 30 min later, the largest aftershock (MJ7.6) occurred around 50 km east-off the Kanto District. A width and amplitude of a main pulse in the transverse component records are 15 s to 20 s and amplitude of up to 30 cm, respectively, in the Boso Peninsula (150 km to 200 km).

Each pulses of the hyper resonance due to Mw9 event are much greater than the main pulse of the MJ7.6 aftershock.

### 3. A resonance of a period of 10 s to 15 s

The second (R-2) is a resonance of a period of 10-15 s, amplitude of 10 cm to 20 cm and duration time of a few minutes in the northern part of the Chiba Pref., where the thickness of the Tertiary sedimentary layer is up to 3 km.

### 4. A resonance of a period of 5 s to 10 s

The third (R-3) is a resonance in the central part of the Kanto basin of a period of 6-8 s, which is so-called the long-period strong ground motion.

### 5. Concluding remarks

We have recognized the distinguished resonances mostly in the Kanto District, triggered by the giant SH waves due to the Mw8.4 super sub-event. Similar resonances due to the largest aftershock are recognized with one-order smaller amplitude. One of common features is that the resonances are remarkable in the transverse component rather than radial and vertical component records.

### Reference

Kawasaki, I., H. Ishii, Y. Asai, and T. Nishimura, 2014, An Mw8.4 super sub-event associated with the 2011 Mw9.1 Tohoku earthquake, *Zisin*, 87-98, in Japanese.

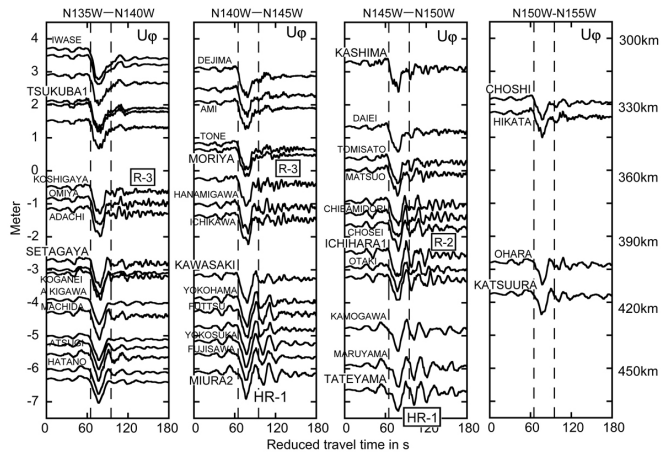
Fig.1 Record sections of transverse component displacement of GPS high sampling data in the Kanto District observed for the 2011 Mw9 Tohoku earthquake. Horizontal scale is a travel time in s reduced by 3.9 km/s. Vertical scales at left and right sides are amplitude and epicentral distance, respectively. HR-1 denotes the hyper resonance of a period of 15-20 s and peak-to-peak amplitude of up to 1 m. R-2 and R-3 denote resonances of periods of 10-15 s and 6-8 s, respectively.

Keywords: hyper resonance, GPS high sampling record, 2011 Tohoku earthquake, Boso Peninsula, Tertiary sedimentary layer

SSS26-07

Room:103

Time:May 26 11:00-11:15





## Stochastic excitation of seismic waves by an intense Hurricane: Seismic excitation proportional to the cube of pressure

TANIMOTO, Toshiro<sup>1\*</sup>

<sup>1</sup>Dept. of Earth Science, UCSB, CA93106, USA

Earthscope Transportable Array (TA) has recorded a few hurricanes that propagated through the network. We report our analysis of Hurricane Isaac in 2012 that provided an opportunity to monitor the interactions between the atmosphere and the solid earth in detail as this hurricane passed through the network; this was possible because TA has both seismometers and barometers and allowed us to examine how seismic ground motions were excited with changing surface pressures. We analyzed data in a low frequency band 0.01-0.02 Hz because we had evidence that the signals are generated by processes near the center of a hurricane.

Surface pressure is the excitation source of seismic signals; it has short correlation length (~1 km or less) whereas excited surface waves (0.01-0.02 Hz) have horizontal wavelengths of 100-300km. The source is also spread over some areas. Under such conditions, we must model the source by a stochastic pressure source that is spread over the surface of the Earth. In terms of parameters, this source is then characterized by two parameters, the pressure power spectral density  $S_p$  and its correlation length  $L$  but both parameters can vary in space. We derived a relation between the observed power spectral density (PSD) of seismic velocity  $S_v$  and the PSD of surface pressure  $S_p$  by the normal mode theory.

For a low frequency range 0.01-0.02 Hz, seismic and pressure amplitudes show, at least to first order, axisymmetric variations and also decreasing trends with distance from the center of a hurricane. Taking the center of a hurricane at the origin and assuming axisymmetry, we can write down an integral relation between  $S_v$  and  $S_p$  as

$$S_v(x) = \int K(x, y) L^2 S_p(y) dy$$

where  $x$  and  $y$  are distances from the center of a hurricane.  $K(x, y)$  is the excitation kernel for a source at  $y$  and a seismic observation at  $x$  and was computed for an Earth model PREM.

From data, we have  $S_v$  and  $S_p$  in the integrand. We first noted that a constant  $L$  cannot make the two observed quantities compatible. Therefore, we introduced the  $y$  dependence in  $L^2$  where the correlation length varied with distance and solved for it. With such spatially varying  $L(y)$ , the two data can be made compatible. The important point is that we also found a correlation between this  $L$  (solution) and surface pressure  $S_p$ . In fact there is a good linear relationship that can be expressed as  $L=c S_p$  where  $c$  is a constant. This is equivalent to saying that  $L^2 S_p$  in the integrand is  $c^2 S_p^3$ .

This relation implies that the excitation of seismic ground motion becomes proportional to the cube of pressure. Near the center of a hurricane, pressure variations generally increase, but seismic-excitation becomes even more efficient near the center because of this nonlinear relation.

Keywords: Stochastic excitation, Hurricane, Atmosphere-Solid Earth interaction

## Receiver function analysis of airgun-OBS survey data for imaging PS converted wave

SHIRAISHI, Kazuya<sup>1\*</sup> ; ABE, Susumu<sup>1</sup> ; ASAKAWA, Eiichi<sup>1</sup> ; FUJIE, Gou<sup>2</sup> ; SATO, Takeshi<sup>2</sup> ;  
KODAIRA, Shuichi<sup>2</sup>

<sup>1</sup>JGI, Inc., <sup>2</sup>JAMSTEC

In marine seismic survey with airguns and multicomponent ocean bottom seismographs (OBS), P-to-S converted waves are frequently observed in common receiver records. S-wave properties in sedimentary basins could be obtained from information such as traveltimes difference between P and S waves. The receiver function (RF) analysis is generally applied to passive seismic records of natural earthquakes for imaging the receiver-side structures. In this study, we attempt to apply the RF analysis to airgun-OBS survey data to extract the PS converted waves, and then image structures of the conversion boundaries.

The RF records are synthesized by deconvolution of multicomponent seismic records. After azimuth correction of the OBS orientation for two horizontal components, nine RF records can be obtained from all combinations of three components. In this study, only two RF records from vertical and radial components are analyzed. Final receiver function records are obtained by stacking over the deconvolved traces and summing the R/Z record and the time reversed Z/R record. Because the OBSs are deployed sparsely in general airgun-OBS surveys, it is difficult to synthesize the continuous seismic section as the multichannel seismic survey. We can just plot the RFs at receiver locations as the receiver-side structures.

We applied the RF analysis to the airgun-OBS survey data acquired by JAMSTEC. In the case in the northwest Pacific, the interval of OBS deployment is 6km and the airgun shot line is 237 km-long. In this area, there is wide and relatively simple sedimentary layers and the change of seafloor surface is very gentle. The final RF section shows clear PS conversion boundary that indicates the basin bottom. That is horizontally traceable and correspondent to the PP reflection boundary on the seismic section by the multi-channel seismic survey. Our result shows applicability of the RF analysis to the airgun-OBS survey data to extract the PS conversion waves and image receiver-side structures. Further analyses are applicable to the RF records to obtain detailed information related to S waves.

Keywords: receiver function, airgun-OBS survey, PS converted wave

## FK-filtering vs. Predictive Deconvolution in the Multiple Reflection Removal Approach

ISCAN, Yeliz<sup>1\*</sup>; LORETO, M.filomena<sup>2</sup>; ZGUR, Fabrizio<sup>3</sup>; OCAKOGLU, Neslihan<sup>4</sup>

<sup>1</sup>Istanbul University Engineering Faculty Department of Geophysical Engineering 34320 Avcilar/Istanbul, <sup>2</sup>Istituto di Scienze Marine Consiglio Nazionale delle Ricerche 40129 Bologna/Italy, <sup>3</sup>Istituto Nazionale di Oceanografia e di Geofisica Sperimentale 34010 Sgonico, Trieste, Italy, <sup>4</sup>Istanbul Technical University Department of Geophysical Engineering Maslak 34469 Istanbul/Turkey

Multiple reflection removal is one of the most important topic in seismic reflection processing, especially in the marine seismic data, where seabed multiple reflections can often severely mask the primary events. It is thus necessary to remove or to attenuate them prior to stack the data. In shallow water, the most common type of multiples is water reverberation.

In this study two different pre-stack attenuation techniques have been tested and compared by using the Focus PARADIGM software package: namely, the FK-filtering and the Predictive deconvolution. We performed this comparison on a multichannel seismic profile acquired offshore W-Calabria (SE Tyrrhenian Sea; Loreto et al., 2012), and characterized by the presence of remarkable multiple reflections.

Coherent linear events within the t-x domain can be separated as dip events within the F-K domain. This allows to remove some undesired energy (such as multiples) from the data. F-K filtering works based on the following strategy. NMO (Normal Move Out) correction is first applied to the Common Mid Point sorted data by using velocity lower than water velocity up to the first seabed multiple occurrence; a velocity close to sea water velocity (or slightly higher) will instead be applied from the first multiple up to the end of the record.

This will result in an overcorrection of the primary events in the t-x domain that consequently will fall within the positive sector of the F-K spectrum. The multiple reflections, conversely, will be either flattened or slightly under corrected, and thus will be positioned in the proximity of the F-K spectrum vertical axes or in its negative sector.

By applying the F-K filter on either the corrected (vertical axis) or undercorrected (negative sector) events, the multiples will be removed leaving untouched the primary events.

Deconvolution is a process whose purpose is to improve the temporal resolution by compressing signals to very short duration wavelets (spiking deconvolution) or to remove, if present, periodic events present in the data (peg lag multiples, bubble effect etc.). In the latter case, we refer to predictive deconvolution that can also be used to suppress seafloor multiple reflection. To perform predictive deconvolution, first the seafloor reflector has been picked on the brute stacked section, and the corresponding time stored within the water depth data header. Later, a dedicated velocity analysis was performed in order to flatten both the seafloor and the related multiple reflections of the first and secondary order. Finally, the deconvolution was applied with by adopting a gap parameter retrieved by the picked water depth, representing in this specific case the predictable occurrence of the first multiple. Compared to the conventional predictive deconvolution, where the gap parameter is kept constant, in the applied deconvolution the water depth changes continuously because it refers to the seafloor depths. Operator length is chosen so as to carefully remove only the multiple reflections and possibly leave untouched the primaries.

The results of F-K filtering and Predictive deconvolution indicate that the predictive deconvolution is more successful both to remove the multiples and to increase the resolution in the shallow part of the section.

### References

Loreto, M. F., et al., 2012. In search of new imaging for historical earthquakes: a new geophysical survey offshore western Calabria (southern Tyrrhenian Sea, Italy). *Bollettino di Geofisica Teorica ed Applicata*, 53(4), 385-401.

Keywords: FK Filtering, Predictive Deconvolution, Multiple Reflection

## Phase of Severe Earthquake of Seismic Wave

NISHIZAWA, Masaru<sup>1\*</sup>

<sup>1</sup>none

### Conclusion

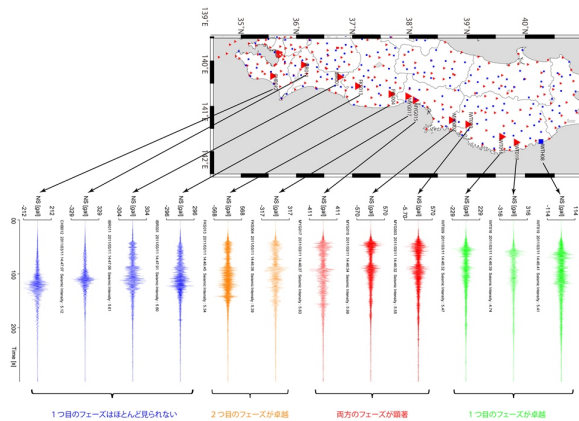
1. Strong motion seismogram exists tajo.  
Was that the reason, present Earthquake Early warning is difficult.
2. A building on the soft ground accept rotation level and up and down by strong motion Earthquake.
3. Phase (shift) is one of the very important fact.

Keywords: Severe Earthquake, Finite Amplitude Wave, Phase

近地強震動波形に見られるフェーズの特徴

「平成23年(2011年)東北地方太平洋沖地震による強震動 pp.6」  
 防災科学技術研究所  
[http://outreach.eri.u-tokyo.ac.jp/ul/EVENT/201103\\_NIED\\_0313.pdf](http://outreach.eri.u-tokyo.ac.jp/ul/EVENT/201103_NIED_0313.pdf)

- ・断層近傍の加速度波形には顕著な2つのフェーズがみられ、少なくとも2つの大きなすべりが示唆される
- ・北では1つ目のフェーズが卓越するのに対し、南では1つ目のフェーズはほとんど見えず2つ目のフェーズのみが見える
- ・これら2つのフェーズは、北および南に位置するすべりに対応すると考えられる
- ・リアルタイム震度の立ち上がり早いものと、遅いものがあるが、いずれのすべりで最大震度が出ているかに対応すると考えられる
- ・2つの顕著なフェーズの中間に、鋭いフェーズが見られる観測点がある(例えばFKS013, FKS004, MYG017, MYG015)
- ・他にも多くのフェーズが見られ、複雑な震源過程が示唆される



## Scattering and intrinsic attenuation in Kyushu

SHITO, Azusa<sup>1\*</sup>; MATSUMOTO, Satoshi<sup>2</sup>; OHKURA, Takahiro<sup>1</sup>

<sup>1</sup>Institute for Geothermal Sciences, Kyoto University, <sup>2</sup>Institute of Seismology and Volcanology, Kyushu University

Attenuation of seismic wave energy is caused by two factors: scattering and intrinsic absorption. The former is the scattering of seismic wave energy due to random heterogeneities in seismic wave velocity and the density of the medium, while the latter is the conversion from seismic wave energy to heat energy by internal friction due to anelasticity of the medium. Quantifying scattering and intrinsic attenuation is important to understanding the structure of the lithosphere in terms of seismotectonic features.

We separately estimate scattering and intrinsic attenuation by applying the multiple lapse time window analysis (MLTWA) technique [Hoshihara et al., 1991]. This technique is based on a comparison between observed and calculated seismic wave energy density obtained using radiative transfer theory in several successive lapse time windows. In the present study, we measure the integrated seismic wave energy as a function of distance and frequency for three consecutive time windows with a length of 15 s following the S-wave onset. The window length is chosen in such a way that the first window contains a significant contribution of the direct S-wave energy and the last two windows mainly contain the contribution of the scattered energy. The observed energy is calculated in three steps. First, we filter the waveforms using a third-order Butterworth band-pass filter at the following frequency bands: 1-2, 2-4, 4-8, 8-16, and 16-32 Hz. Second, we obtain the envelopes by taking the sum of squares sum of the three-component amplitudes of filtered waveforms. Third, we integrate the root mean square amplitude of the envelopes in the three time windows. By comparing the observed and calculated energy distributions in terms of the misfit function, we obtain the best pair of scattering and intrinsic attenuation. We use the Levenberg-Marquardt algorithm, a non-linear least squares fitting procedure, to find the minimum of the misfit function.

We estimate the scattering and intrinsic attenuation in Kyushu, which is the site of active volcanoes and seismic activity within the Beppu-Shimabara rift valley and elsewhere. We collect waveform data from the Hi-net network operated by NIED. During the period from 2004 to 2014, we choose 180 earthquakes with magnitudes ( $M_{jma}$ ) of 0.5-3.5 and with depths of <20 km. We select event station pairs with epicentral distances of <100 km recorded at 78 Hi-net stations.

In all the studied area, intrinsic absorption dominates over scattering loss at low frequencies (1-2 Hz), whereas scattering loss predominates at high frequencies (16-32 Hz). The results show strong spatial variations in scattering and intrinsic attenuation that depend mainly on the tectonic setting. For frequencies of 1-2 Hz, areas with strong scattering loss correspond mainly to the locations of the volcanoes, while areas with strong intrinsic absorption correspond to the locations of volcanoes and active faults, which are marked by low-velocity anomalies.

Keywords: crust, scattering attenuation, intrinsic attenuation

## Small-scale velocity heterogeneity of subducting oceanic crust inferred from high-frequency trapped P and S waves

TAKEMURA, Shunsuke<sup>1\*</sup>; YOSHIMOTO, Kazuo<sup>1</sup>; TONEGAWA, Takashi<sup>2</sup>

<sup>1</sup>Yokohama City University, <sup>2</sup>Japan Marine Science and Technology

### Observed characteristics of high-frequency trapped waves

Observed records during earthquakes occurring at depth of 50-60 km at southwestern Ibaraki, central part of Japan, are characterized by distinct trapped P and S waves (Hori, 1990, 2006). From detailed analysis of Hi-net waveform at Kanto-Tokai region, we found significant distorted trapped P and S waves, characterized by strong peak delay and spindle-shape envelope, at stations where the Philippine Sea Plate (PHS) exists at depths of 10-15 km. On the other hand, pulse-like trapped signals were observed at other region. These results indicate that spindle-shape trapped signals may be caused by shallower heterogeneous structure of the oceanic crust of the PHS.

### Simulations of seismic wave propagation

To clarify the cause of strong peak delay of trapped waves, we conduct finite-difference method (FDM) simulation of seismic wave propagation in the 2-D heterogeneous structures of two profiles. Observed seismograms along each profile were characterized by spindle and pulse-like trapped waves, respectively. Our 2-D simulation model is covering the zone 245 by 123 km, which has been discretized with grid size 0.015 km. We assumed the layered background velocity structure base on the JIVSM proposed by Koketsu et al. (2008).

To introduce the effects of seismic wave scattering, we assumed small-scale velocity heterogeneities in each layer referred from Table 4 of Takemura and Yoshimoto (2014). Because of spindle-shape waveforms, we employed strong small-scale velocity heterogeneities in the oceanic crust, which is characterized by a Gaussian power spectral density function (PSDF) with correlation length of  $a = 1$  km and root-mean-square value of  $e = 0.07$  superposed on an exponential PSDF with  $a = 3$  km and  $e = 0.07$  (Takemura and Yoshimoto, 2014). Recently, Takemura et al. (2014, SSJ; 2015) reported that velocity increase in the subducting oceanic crust layer 2 of the PHS due to dehydration reactions at depths of 30-40 km occur and consequently the oceanic crust at depths below 40 km becomes a homogeneous layer. Therefore, we simply assumed that small-scale velocity heterogeneities in the oceanic crust simultaneously disappear with velocity increase in oceanic crust layer 2 at a depth of  $Z_D$ . We conducted FDM simulations changing this depth  $Z_D$  (30, 40 and 50 km) in the both profiles.

Simulation results with  $Z_D = 40$  km well reproduced both pulse-like and spindle-shape trapped P and S waves along each profile. Structural change in the subducting oceanic crust due to dehydration might occur at a depth of 40 km.

### Shallower structure of oceanic crust

In the profile with spindle-shape trapped waves, because the PHS exits at depths of 10-15 km, trapped waves propagate along the shallower heterogeneous oceanic crust without energy release into the lower crust and consequently strong peak delay of trapped waves occur.

Shallower oceanic crust before dehydration is considered to be characterized by rich hydrous minerals. Thus, small-scale velocity heterogeneities in the oceanic crust may be related with fluid in the oceanic crust.

### Acknowledgement

We acknowledge the National Research Institute for Earth Science and Disaster Prevention, Japan (NIED) for providing the Hi-net waveform data and F-net CMT solutions. The computations were conducted on the Earth Simulator at the Japan Marine Science and Technology (JAMSTEC).

Keywords: Seismic wave propagation, oceanic crust, small-scale heterogeneity, seismic wave diffraction and scattering, numerical simulation

## Frequency and distance changes in the apparent P-wave and S-wave radiation pattern

KOBAYASHI, Manabu<sup>1\*</sup> ; TAKEMURA, Shunsuke<sup>1</sup> ; YOSHIMOTO, Kazuo<sup>1</sup>

<sup>1</sup>Yokohama City University

### **Introduction**

When earthquake occurs in a homogeneous medium, the spatial variation of maximum amplitude (apparent radiation pattern) of S waves is characterized by four-lobe pattern, which has larger S waves in the direction of fault strike and its normal direction. However, some studies pointed out that the apparent S-wave radiation pattern is significantly distorted for frequencies higher than 3-5 Hz and showing almost isotropic pattern rather than four-lobe pattern (e.g., Liu and Helmberger, 1985; Takemura et al., 2009). Recently, by using dense Hi-net waveform data, Kobayashi et al. (2014, SSJ) reported that the apparent P-wave radiation pattern is also distorted at high frequency. In this study, to investigate the differences of propagation features between P and S waves, we examined frequency and distance changes in both apparent P- and S-wave radiation patterns based on the method proposed by Kobayashi et al. (2014).

### **Data and Method**

We used 755 velocity seismograms recorded at Hi-net stations with hypocentral distances of 0-150 km during 10 shallow crustal earthquakes that occurred in Chugoku region, southwestern Japan. Earthquakes in this study were characterized by strike-slip faulting mechanism. Based on a method of Kobayashi et al. (2014), we evaluated the azimuthal change in amplitude fluctuations of P and S waves, which were calculated by fluctuation of amplitude from master attenuation curves estimated by the coda normalization method (e.g., Yoshimoto et al., 1993). We also evaluated the theoretical fluctuation by calculating fluctuation of theoretical radiation pattern coefficient from its average at a certain hypocentral distance (Aki and Richards, 2002, Ch. 4). To quantify how the apparent radiation pattern is distorted, we calculated the cross-correlation coefficient (CCC) between observed and theoretical amplitude fluctuations for each frequency and distance. The frequency bands in our analysis were 0.5-1 Hz, 1-2 Hz, 2-4 Hz, 4-8 Hz, and 8-16 Hz.

### **Frequency and distance changes in the apparent radiation pattern**

Data analysis demonstrated that the four-lobe P- and S-wave apparent radiation patterns were preserved at low frequency (0.5-1 Hz), but those were gradually distorted with increasing frequency and distance. The cause of such observation might be the seismic wave scattering due to the small-scale velocity heterogeneity along propagation path. At high frequency (8-16 Hz), the apparent radiation pattern was significantly distorted even for short hypocentral distances (40 km). It might be suggested that this observation reflects the effects of scattering due to localized strong heterogeneities around source region and/or the complexity of source rupture process.

The distortion of the apparent S-wave radiation pattern was stronger than P wave for all frequencies and distances. Furthermore, even for source region, the CCC values of S waves were obviously smaller compared with P waves. The values of CCC of P and S waves at distance of 0 km for frequency 2-4 Hz were 0.75 and 0.55, respectively. These results imply that the effects of localized heterogeneities around source region and/or source rupture complexity on P and S waves might be significantly different.

### **Acknowledgement**

We acknowledge the National Research Institute for Earth Science and Disaster Prevention, Japan (NIED) for providing Hi-net/F-net waveform data and the CMT solutions from F-net. We also used the unified hypocentral catalog provide by the Japan Meteorological agency (JMA).

Keywords: Radiation pattern, Body wave, Wave propagation, Wave scattering and diffraction

## Comparison between ray theory and synthetic seismograms for transversely isotropic media

BORGEAUD, Anselme<sup>1\*</sup> ; KONISHI, Kensuke<sup>1</sup> ; GELLER, Robert J.<sup>1</sup> ; KAWAI, Kenji<sup>2</sup>

<sup>1</sup>Department of Earth and Planetary Science, Graduate School of Science, University of Tokyo, <sup>2</sup>Department of Earth Science and Astronomy, Graduate School of Arts and Sciences, University of Tokyo

Imaging seismic anisotropy is essential for a better understanding of geodynamics, since it provides information on deformation and flow in the crust and mantle. S-wave splitting has been widely used to infer the presence and extent of anisotropy. The inference of anisotropy from S wave splitting relies, however, on ray theory, which is strictly valid only for infinitely high frequencies, and thus may not accurately reflect real finite-frequency seismic data. For example, a recent study by Komatitsch et al. (2010) showed that splitting of diffracted S waves in the D'' region, just above the CMB, is present in synthetics computed for an isotropic velocity model. In this study we compute travel times for a transversely isotropic (TI) medium using a newly developed software package (Konishi et al., JpGU, 2015). We then compute full-wave synthetics using the Direct Solution Method (DSM; Kawai et al., 2006). We focus on two regions of the mantle: D'' and the upper mantle. We confirm apparent S-wave splitting in synthetics computed for the isotropic IASP91 velocity model for epicentral distances over 100 degrees, in agreement with the results of Komatitsch et al. (2010). We also compare the predictions of geometrical optics to synthetics for TI models for phases which sample the upper mantle and the D'' region.

Keywords: DSM, Travel time, D double prime, Upper mantle, Anisotropy, S-wave splitting



## Amplitudes of sP depth phase observed at small epicentral distances from offshore events in the northeastern Japan

KOSUGA, Masahiro<sup>1\*</sup> ; KATO, So<sup>1</sup>

<sup>1</sup>Grad. Sch. Sci. & Tech., Hirosaki Univ.

Travel times of sP phase have been widely used to improve depth accuracy of earthquakes for both far- and near-field observations. However, the amplitudes of sP phase has not been paid much attention probably because the amplitudes may depend on many parameters. Here we developed an automated technique to detect sP phase and measure its amplitude to search for future use of amplitude data. The method consists of the picking of possible arrival times for each station, screening data through depth relocation, and amplitude correction. The first step picks possible pairs of arrival times and amplitudes in the time windows that satisfy the criteria of polarization characteristics. The combined data from all stations are organized into several groups based on the relation between sP-P times and epicentral distance. The screening process selects the best group that gives the least travel time residuals from the event depth revised by sP-P times. Finally, the amplitudes are corrected for the dependence on epicentral distance. We applied the method to a data set from offshore earthquakes of the northeastern Japan. The amplitudes plotted on focal sphere are partly consistent with the CMT solution. The spatial distribution of amplitudes plotted at reflection points show complex pattern that suggest no significant correlation with the submarine topography. Thus the amplitude of sP phase probably reflects source radiation, together with some additional factors such as spatial heterogeneities of reflectivity. This result suggests potential use of sP amplitude to constrain the focal mechanisms of offshore earthquakes.

Keywords: sP wave, reflection, amplitude, focal mechanisms

## ”AnisoTime” Travel time computation software for transversely isotropic media.

KONISHI, Kensuke<sup>1\*</sup> ; BORGEAUD, Anselme<sup>2</sup> ; GELLER, Robert<sup>2</sup> ; KAWAI, Kenji<sup>3</sup>

<sup>1</sup>Academia Sinica, <sup>2</sup>Graduate School of Science, University of Tokyo, <sup>3</sup>Graduate School of Arts and Sciences University of Tokyo

Software for computing body-wave travel times is necessary in work on many seismological research problems. The TauP toolkit (Crotwell et al., 1999) is widely used for isotropic laterally homogeneous media. The basic theory for travel times in transversely isotropic (TI) media was presented by Vlaar (1968), 1969; Woodhouse, 1981), but, to our knowledge, free software for making travel time calculations for the TI laterally homogeneous case has not heretofore been available. We have developed such a package, which we call ”AnisoTime.” The beta-test version is available at <http://www-solid.eps.s.u-tokyo.ac.jp/~dsm/>.

Keywords: Travel time, anisotropy

## Simulation of the seismic wave propagation on the tablet computer

EMOTO, Kentaro<sup>1\*</sup>

<sup>1</sup>Graduate School of Science, Tohoku Univ.

Smartphones and tablet computers are widely used in recent years. Some of those devices have the high-performance CPU and large memory size, which comparable to the PC several years ago. Convenience and intuitive operation are merits of using the tablet computer compared to the desktop PC. In this study, I examine the possibility of the numerical simulation on the tablet PC and create the application to easily simulate the seismic wave propagation. I use the iPad Air as a target.

I consider the seismic wave propagation in 2D. By using the finite difference method with a staggered-grid technique, I solve the equation of motion of elastic body. For the simplicity, the accuracy is 2nd-order in both time and space. The medium consists of four layers including an air layer. The grid spacing is 200m in both horizontal and vertical directions, and the number of the grid points are 512 and 384 in the horizontal and the vertical direction, respectively. That is, the simulation area is 102km wide and 77km deep. The time step is 10ms. In order to decrease user frustration and create the interactive user interface, I simultaneously draw the wave field and calculate the wave propagation rather than playing the video after the simulation. Here, I draw the wave field in every 20 steps (0.2s). I calculate the divergence and the rotation and draw the amplitude of the P and S waves as the wave field. I don't draw the amplitude in pixel by pixel, because it takes too much time. I make a picture of the wave field on the memory and then draw it on the screen. I also plot the seismogram at an arbitrary station. As one of the intuitive operation, layer boundaries and locations of the station and the source are movable by the finger. I set ten points on each layer boundary. The boundary is defined by those movable points. Although the velocity of each layer is fixed, the user can make various settings of the simulation intuitively. For the advanced simulation, the user can introduce the random fluctuation of the velocity in each layer. The user can change the spatial spectrum of the fluctuation intuitively by the finger and arbitrarily change the size of the fluctuation.

Even when I double the number of the grids in both horizontal and vertical directions, I can simulate the wave propagation without any memory problem. However, simulating up to 10s takes close to three minutes. Before I extend the area, it takes only 40s. The wave field is updated in every 0.2s, so the total number of the update is 50 times for the simulation up to 10s. Therefore it takes more than 1s to update the wave field. It is too slow and leads to the frustration of the user. For the tablet computer, the light performance is required. If I shorten the rate of the update such as 0.1s, the interval of the update of the wave field is also becomes short. However updating the image of the wave field becomes heavy load, so the user isn't satisfied the speed of the simulation. The size of the image rather than the resolution of the image is also one of the main load of the application.

We can perform the 2D seismic wave propagation on the iPad. By using the tablet computer, we can simulate it interactively and intuitively. It is useful to explain the seismic wave propagation for non-specialist users.

Keywords: mobile application, seismic wave propagation, simulation, iOS

## Estimation of velocity change depth from wave-propagation simulation and interferometric analysis of Hi-net and KiK-net

SAWAZAKI, Kaoru<sup>1\*</sup> ; UENO, Tomotake<sup>1</sup> ; SHIOMI, Katsuhiko<sup>1</sup> ; SAITO, Tatsuhiko<sup>1</sup>

<sup>1</sup>National Research Institute for Earth Science and Disaster Prevention

Since Hi-net and KiK-net sites are co-located, we can detect the depth dependence of seismic velocity change by applying the interferometric analysis to seismograms recorded by these two types of seismograph networks. In this study, we measure auto-correlation function (ACF) of ambient noise record obtained by Hi-net, and measure deconvolution function (DCF) of the surface and the borehole-bottom seismograms obtained by KiK-net for the Myoko-Kogen station (N.MKGGH/NIGH17). By comparing these two functions, we detect the depth dependence of seismic velocity change associated with the  $M_W$ 6.3 earthquake occurring on November 22, 2014 at northern part of Nagano-prefecture, Japan. By applying the interferometric analyses, we detect velocity reduction ratios of 1-2 % and 3-4 % for the ACF of Hi-net record and for the DCF of KiK-net records, respectively, within the time period of one week after the mainshock. This difference in the velocity reduction ratios could be attributed to difference in sensitivity of the two functions; the DCF is sensitive to change in the medium above the borehole-bottom receiver (0-150 m depths), while the ACF is sensitive to wider zone. Next, we perform a two-dimensional finite-difference wave propagation simulation and examine the change of ACF associated with the 3 % velocity reduction at 0-150 m depths considering the result revealed from the DCF of KiK-net records. The reference velocity structure used in this simulation is created by adding random fractional fluctuations to the depth-averaged velocity structure obtained from the seismic tomography data around the target region. The velocities of the top layer are set to  $V_P = 4.0$  km/s and  $V_S = 2.0$  km/s for model 1, and  $V_P = 3.0$  km/s and  $V_S = 1.0$  km/s for model 2. The velocities between the top layer and the 2.5 km depth are smoothly interpolated and connected to the tomography data. The positions of source and receiver are co-located at the 150 m depth. Applying the stretching technique to the simulated waveforms, we obtain 0.7 % and 1.2 % velocity reduction ratios in average for the models 1 and 2, respectively. According to the well-logging data at Myoko-Kogen station, the average velocities at 0-150 m depths are  $V_P = 1.8$  km/s and  $V_S = 0.6$  km/s, which are slower than the velocities of the top layer adopted for the model 2. Therefore, the true velocity reduction ratio would be larger than 1.2 % if a realistic velocity structure is available for the finite-difference simulation. This result indicates that over half of the observed velocity reduction ratio detected by the ACF of Hi-net record is attributed to the velocity reduction at the top 150 m depths.

Keywords: Hi-net, KiK-net, interferometry, velocity change, finite-difference simulation

## Ground Motion Prediction of Finite Rupture Subduction Earthquakes using the Ambient Seismic Field

VIENS, Loic<sup>1\*</sup> ; KOKETSU, Kazuki<sup>1</sup> ; MIYAKE, Hiroe<sup>1</sup> ; SAKAI, Shin'ichi<sup>1</sup> ; HIRATA, Naoshi<sup>1</sup> ;  
HONDA, Ryou<sup>2</sup>

<sup>1</sup>Earthquake Research Institute, University of Tokyo, <sup>2</sup>Hot Springs Research Institute of Kanagawa Prefecture

The ever-increasing construction of large-scale structures such as high-rise buildings, oil tanks, and suspension bridges requires an accurate prediction of long-period ground motions (4-10 s) for seismic hazard assessment. The slow attenuation with distance of the long-period ground motions combined to possible amplification in sedimentary basins can lead to large damages as those observed during the 1985 Michoacan earthquake ( $M_w$  8.0) where more than 1000 buildings were destroyed in the Mexico city located at more than 300 km from the hypocenter. We focus this study on the Kanto basin where the Tokyo city is located. In the basin and its surrounding, more than 600 stations composed of 3 component seismometers recording continuous data have been selected. These stations are a part of different networks including the Metropolitan Seismic Observation network (MeSO-net), Hi-net and F-net of NIED, the Japan Meteorological Agency (JMA) network, and the Hot Spring Research Institute of Kanagawa Prefecture network. Stations located above the 1923 Kanto earthquake rupture area have been considered as virtual sources and others as receivers. Deconvolution method has been applied between every virtual source and the receivers to extract single force impulse response functions for each pair of stations. As only relative, rather than absolute, amplitude can be extracted with this technique, we calibrated the impulse response function amplitudes using records of a moderate shallow earthquake ( $M_w \sim 5$ ) that occurred close to the virtual sources. Once the amplitude scaled, we show that both impulse response functions and earthquake records have similar phase and amplitude in the period range of 4 to 10 s. Then, we built finite rupture models for  $M_w \sim 7$  subduction earthquake scenarios that we discretized in subfaults. For each station considered as a receiver, we show that it is possible to interpolate the calibrated impulse response functions extracted between every virtual source and the receiver to obtain one impulse response function for each subfault. We also took into account the depth and the dip angle of the fault and the rupture propagates radially with a speed of 2 km/s. We confirm that peak ground velocities and durations of our simulated ground motions are strongly amplified in the Kanto basin.

Keywords: Long-period ground motion prediction, Finite rupture subduction earthquakes, Ambient seismic field, Seismic interferometry, Kanto basin

## Application of seismic interferometry to waveforms of small vibration recorded by the existing seismometer of a dam

SEIICHIRO, Kuroda<sup>1\*</sup> ; TAGASHIRA, Hidekazu<sup>1</sup> ; MASUKAWA, Susumu<sup>1</sup>

<sup>1</sup>NARO, National Institute for Rural Engineering

The existing seismometers installed at the dams for irrigation have recorded many seismic records during huge earthquake events. Those are useful for analysis to understand how dams behaved during earthquake. Those records are valuable as the evidence not only to show the behavior of dams caused by but also to retrieve the index to reflect the dynamic property of the dams. Considering this point, we have applied the concept of seismic interferometry and its method to seismic records of the dams to estimate their properties of seismic wave propagation and the dynamic properties of those structures.

This shows the applicability of seismic interferometry for small vibration records of existing seismometer of dams, like small earthquake records, whose maximum acceleration are less than  $1\text{cm/s}^2$ , or ambient noise. Based on the analysis for the waveform of acceleration during more than 10hours, we can retrieve the waveforms of time domain response similar to the one extracted from the seismic record of earthquake events, whose maximum acceleration is more than  $2\text{cm/s}^2$ , from small earthquake records and even from ambient noise only. This fact shows the proposed method might be applicable more frequently, if we applied it not only earthquake records but also the small records which has been considered to be trivial ones.

Though we must verify the applicability of this method to the other many dams, this method might be expected to be more useful in an area where the earthquake frequency is very small, or at a dam site where the seismometer has been installed recently and obtained little or not enough seismic records yet.

Keywords: sam for irrigation, seismometer, seismic waveform, seismic wave propagation, seismic interferometry, soil structure

## Temporal changes of seismic velocity in Tokai area revealed by the observation of the Toki seismic ACROSS signals

KUNITOMO, Takahiro<sup>1\*</sup> ; YAMAOKA, Koshun<sup>1</sup> ; WATANABE, Toshiki<sup>2</sup>

<sup>1</sup>Graduate School of Environmental Studies, Nagoya Univ., <sup>2</sup>ERI, Univ. of Tokyo

We report on the travel time changes of the seismic ACROSS signals observed by Hi-net stations in Tokai region from 2008 to 2014, especially after the Tohoku Earthquake (March. 11, 2011, M9.0), and overview seismic velocity changes in the earth's crust in the Tokai region for 7 years.

Acknowledgement: Hi-net data are provided by National Research Institute for Earth Science and Disaster Prevention, Japan (NIED). Toki ACROSS transmitting station is managed by Japan Atomic Energy Agency (JAEA).

Keywords: seismic ACROSS, seismic velocity change, travel time change, Hi-net

## A simple method to improve automatic CMT solutions based on a feature of long-period seismic wavefields

SAKAI, Takahide<sup>1\*</sup> ; KUMAGAI, Hiroyuki<sup>1</sup> ; PULIDO, Nelson<sup>2</sup> ; NAKANO, Masaru<sup>3</sup>

<sup>1</sup>Nagoya University, <sup>2</sup>NIED, <sup>3</sup>JAMSTEC

A correct and rapid centroid moment tensor (CMT) estimation of an earthquake is essential to a prompt response of the earthquake and tsunami disaster. Broadband seismograph networks were deployed for the earthquake and tsunami warning in the Philippines and Indonesia, and the long-period (50-100 s) seismic records from that networks are routinely analyzed by the waveform inversion method of SWIFT (Nakano et al., GJI, 2008) to automatically determine CMT solutions. Non-seismic long-period noisy waveforms occasionally appear in the seismic records when seismic waves arrive at stations. These noisy waveforms have relatively larger amplitudes than the seismic waveforms of each event and affect the automatic CMT solutions. However, there is no established way to correct or avoid the noisy waveforms. In this study, we developed a simple and rapid method to detect the noisy waveforms for automatic CMT inversion analysis.

We used the source amplitude defined as the maximum amplitude of an earthquake at each seismograph station corrected for the geometrical spreading and medium attenuation assuming a surface wave. We compared the source amplitudes with the moment magnitudes ( $M_w$ ) of the CMT solutions to distinguish noisy waveforms from seismic waveforms. We carried out numerical tests using synthesized seismograms to investigate the cause of the relationship between source amplitudes and  $M_w$ . In the tests, we used two different source mechanisms and synthesized seismograms at broadband seismic stations in the Philippines as well as grid positions with about 55 km intervals.

We compared the source amplitudes with  $M_w$  in the manual solutions of earthquake that occurred around the Philippines and Indonesia. Although the source amplitudes varied due to the radiation pattern, we found that the variations of source amplitudes fell within a constant band against the change of  $M_w$  in the manual solutions. We calculated the ratios of the individual source amplitudes to the minimum source amplitude in each event. We found that the ratios were less than 10 for most of these events. Therefore, we introduced a threshold in the ratios ( $R$ ) around 10 to detect pulse-like waveforms, and performed the waveform inversion without such waveforms for 25 events with inappropriate automatic solutions. We found that the source locations assuming  $R=11$  best matched with those of the manual solutions and  $M_w$  and source mechanisms also greatly improved. The numerical test results showed that the variations of source amplitudes become larger as the angles between stations and node directions are smaller. This relation may appear if the station density is higher. Therefore, we investigated the variations of source amplitudes and their ratios in the Japan broadband seismograph network (F-net), which is denser than the Philippine network. We found that the variations of source amplitudes fell within a constant band against the change of  $M_w$  and the ratios were less than 10 for most of events with  $M_w$  in the range from 4 to 8.

Our method may be useful to detect noisy waveforms and avoid them in automatic CMT inversion analysis to improve the accuracy of automatic solutions. The ratios were less than 10 in the observation data from the Philippines and Indonesia networks and F-net, of which the station densities are different. This result indicates that the variations of source amplitudes are independent of the density of the stations, and implies that the radiation pattern may be distorted by source complexity and structural inhomogeneity in the long-period seismic wavefields.

Acknowledgements: We used broadband seismic data from F-net of NIED in this study.



## From seismic waveforms to seismic wavefield: A feasibility study of the seismic gradiometry applied to the Hi-net array

MAEDA, Takuto<sup>1\*</sup> ; NISHIDA, Kiwamu<sup>1</sup> ; TAKAGI, Ryota<sup>1</sup> ; OBARA, Kazushige<sup>1</sup>

<sup>1</sup>Earthquake Research Institute, UTokyo

### Introduction

The high-sensitive seismograph network (Hi-net) operated by NIED, Japan equipped with nearly 800 velocity-type seismographs of natural frequency 1 Hz with average separation of 20 km. Although its main target of observation is small, high-frequency seismic waves, it also can act as an ultra-dense long-period seismograph array in particular for large earthquakes because of the wide dynamic range and high S/N of the observation system [Maeda et al., 2011, 2014]. In such long period band, station separation is shorter than the wavelength. Thus, it is expected that they bring us the 2D complex wavefield rather than independent seismic wave traces at individual stations.

Recent advances of the seismic gradiometry method (hereafter referred to as SG) and its successful applications report that we can measure the spatial variation of geometrical spreading and radiation pattern, in addition to the slowness vector from the dense array data [Langston, 2007a,b,c; Liang and Langston, 2009]. In this study, we attempted to assess the feasibility of applying the SG to the Hi-net array to extract complicated wave propagation properties.

### Seismic Gradiometry

The SG first estimates the wave amplitude and its spatial derivative coefficients from discrete station record by the Taylor series approximation and an inverse problem. Then, by assuming the incoming wave packet is constituted by plane wave having spatially varying amplitude term, the slowness vector and spatial derivative of the amplitude term are estimated. The latter term corresponds to the geometrical spreading and radiation pattern. It is a remarkable feature of the SG to separate the amplitude variation due to between wave propagation and other effects.

### Application to the Hi-net

We applied the SG with synthetic data at the actual Hi-net station layout. The synthetic data has the Gaussian function in time with phase speed of 3 km/s, having geometrical spreading reciprocal to the square root of the horizontal distance, and the four-lobed radiation pattern. This synthetic wavefield has a wavelength of about 60 km, which corresponds to the surface waves at the period of about 20 s. The time series at locations of the Hi-net stations were used to as the synthetic data of the numerical experiment. At equally spaced grid points, the wave amplitude and its derivatives are estimated by using the data at nearby stations with distance is shorter than 50 km by the least square. We here note that the least square is always well-posed, inverse matrices to solve the inverse problem can be calculated in advance. Comparing the analytic solution, it was found that the wavefield and the derivatives are quite well estimated with maximum relative errors of about 5% and 10%, respectively. The slowness vector, the radiation pattern and the geometrical spreading terms are estimated by the wavefield and its spatial derivatives at every grid point. The estimated direction of the wave propagation well fitted to the azimuth from the assumed epicenter, and the radiation pattern shows significant variation at around the null axis.

Our preliminary results suggest that the SG method well suite to the band-broaden Hi-net seismograph to extract wavefield behavior at the periods longer than 20 s. This method is appealing that it can estimate the arrival directions at spatially homogeneous grid, and that it can extract amplitude variation not due to simple wave propagation such as radiation pattern. It is promising to obtain spatial phase velocity variation from direct waves, and to grasp wave packets originated from scattering from later coda, to applying the SG to Hi-net dense array data.

Keywords: seismic wavefield, broadband, surface waves, arrival direction